Femtosecond and picosecond ablation of aluminum for synthesis of nanoparticles and nanostructures and their optical characterization

Syed Hamad,[a] G Krishna Podagatlapalli,[b] S. Sreedhar,[b] Surya P. Tewari,[a,b] S. Venugopal Rao [b,*]

[a] School of Physics
[b] Advanced Center of Research in Higher Energy Materials **(ACRHEM)**
University of Hyderabad, Hyderabad 500046, India.

***** Author for correspondence: **svrsp@uohyd.ernet.in**

ABSTRACT

In this paper we report the fabrication of nanoparticles and nanostructures through the interaction of ultrashort (~40 fs) and short (~2 ps) laser pulses with bulk Aluminum immersed in various liquid media of different polarity [chloroform which is polar, carbon tetrachloride which is non-polar, water which is polar, dichloromethane (DCM) which is polar, and Cyclohexane which is non-polar] using the laser ablation technique. Except water and Cyclohexane, other media showed yellow coloration after ablation took place indicating formation of nanoparticles in the solution in both fs and ps domains. The coloration of the laser exposed portion in the Al substrate was golden yellow and its closer view depicted micro-grating (~1-2 μm) and nano-ripple (period 330 nm) formation depending on the focal conditions. The investigation of polarization dependence on the ablation was performed for water media. Depending on the ablation threshold, we observed micron sized structures and nano-ripples on the surface. As the rate of ablation depends on the position of the focus on the Al substrate and beam waist parameters, we have studied the liquid level dependence of ablation with different water levels on the Al substrate and we compared these patterns obtained below, near, and above the ablation thresholds of the sample. Field Emission-Scanning Electron Microscope (FE-SEM), UV-Vis absorption spectra, Electron Diffraction Pattern and Transmission Electron Microscope (TEM) were used for the characterization and comparison of products in both domains.

Keywords: femtosecond, picosecond, Aluminum, ablation, nanoparticles, nano-ripples, microstructure

INTRODUCTION

Metal nanostructures are known to exhibit distinct optical characteristics, which differ from those observed in the bulk and form the basis for a variety of spectroscopic techniques such as surface enhanced Raman scattering (SERS) and second harmonic generation (SHG)[1-5]. Nanoparticles synthesis, nanostructure formation and their characterizations are of great interest because of the physics associated with them and are described by the intermediate regime between quantum physics and classical physics[6]. The electronic properties of the nano-sized systems change dramatically since the density of states and spatial length scale of electronic motion are reduced with decreasing size. For these nano-entities, Eigen states are determined by the systems boundaries and hence the surface effects become very important[7]. Femtosecond (fs) laser ablation (FLA) of metals immersed in liquid environment is the best method among all other methods to generate impurity free nanoparticles of narrower size distribution with reduced porosity[8] and nanostructures of different sizes. Furthermore, as generated nanoparticles remains in the liquid in which ablation takes place, it can reduce the contamination of the surrounding air medium from the expulsion of generated nanoparticles into it. This technique provides the possibility of generating a large variety of NPs those are free of both surface-active substances and counter ions.[9, 10] If the input laser energy density is high enough than damage threshold of metal used, then the deposition of high energy density through an ablation of a fs laser pulse on a metal immersed in liquid results in rapid heating of the surface to high temperatures since the peak intensity of fs laser pulse is so high, and hence eventually it leads to plasma formation. [11] Under suitable high laser fluences, surface of the target melts, and the melt is subsequently dispersed in the surrounding liquid and

Synthesis and Photonics of Nanoscale Materials IX, edited by Frank Träger, Jan J. Dubowski, David B. Geohegan,
Proc. of SPIE Vol. 8245, 82450L · © 2012 SPIE · CCC code: 0277-786X/12/$18 · doi: 10.1117/12.906962

formation of nanostructures take place on the substrate. This structure formation was because of the recoil pressure of the vapor of the liquid which surrounds the laser beam waist at the focus on the surface of the target. In this process along with nanoparticles, free atoms, ions and target fragments will come from the plume. When a metal passes through a melt state due to ablation, stimulation of the physicochemical processes of interaction of metal with liquid medium takes place causing the formation of more complex structures instead of usual spherical particles. The growth of nanoparticles and aggregation takes place under the influence of surrounding liquid environment and aggregation depends upon the permittivity and the polarity of the molecules of the surrounding liquid medium [12]. At fluence close to the melting threshold of the material, short laser pulses with duration of less than 1 nanosecond melt only the micro protrusions on the target surface, giving rise to efficient formation of nanostructures.Under these conditions, the viscous interaction of the vapor of the liquid on the target surface with molten target layer may be responsible for several instabilities like Kelvin-Helmholtz or Rayleigh-Taylor instabilities. These instabilities are tentatively assigned to the observed nanostructure formation on the substrate [13]. One more condition to fabricate nanostructures on the metal surface is the existence of an initial roughness of the target surface since no nanostructures are formed on the optically polished metals [14]. Al is the cheapest metal among the plasmonic metals such as Au, Ag, and it has low melting point (660 ^{0}C) in comparison with other metals, Al nanoparticles can be easily generated. Furthermore Al nanoparticles have large surface area to volume ratio and these are the important fuel in high energetic material applications like propellants, munitions and pyrotechnics and can be used as additives for plastics, and powder metallurgy.[15] Al NPs provide enhanced heat release during their exothermal oxidation. The rate of reactivity increases as the size of Al NP decreases i.e. bare Al is highly reactive. Al is highly reactive to ambient oxygen, pure Al nanoparticles fabrication is restricted by the unwanted oxidation effects which in turn reduce the burn rate and hence the velocity of detonation. Thus the reactivity of the Al nanoparticles diminishes with thin oxide cladding present on it. This effect becomes more pronounced as particle size decreases, since the oxide layer represents a significant fraction of its mass .In this context, femtosecond laser pulses are helpful in quenching of nanostructured Al and thus preserve its metallic nature as it is due to the shorter time of interaction with liquid environment. In order to avoid the instantaneous oxidation caused by the dissolved oxygen in liquids, we have chosen CCl_4, $CHCl_3$ and DCM, since one of the barriers for bare Al NPs formation is the dissolved oxygen in the medium in which ablation takes place. In this paper we report the nanoparticles and nanostructuring of bulk Al in liquids of carbon tetrachloride, chloroform and water under the action of ~40 fs and ~2 ps pulses and, DCM and Cyclohexane with ~40 fs.

EXPERIMENT

Pure Al targets were washed with acetone after sonication to remove organic dopants from the surface. This study (Figure I) has been done by a chirped pulse amplified (CPA) of Ti:sapphire laser system (LEGEND, Coherent) delivering nearly bandwidth limited laser pulses (~40 fs and ~2 ps with 1 kHz repetition rate) at same wavelength of 800 nm as the excitation source. Figure 1 shows the schematic of the experimental setup. The amplifier was seeded with ~15 fs (55-60 nm FWHM) pulses from an oscillator (MICRA, Coherent, 1W, 80 MHz, 800 nm). The average power after the fs amplifier and ps amplifier was 2.5 W and 2 W, respectively. The target was placed into a Pyrex cell and covered by a layer of absolute liquids – water, CCl_4 and $CHCl_3$. After ensuring the sample was perfectly parallel to the optical bench, laser pulses were allowed to focus onto the Al sample using a plano-convex lens of focal length 8 cm. Initial beam polarization used was S-polarization. To get the control over the polarization and the energy of the laser beam, we used the combination of quarter wave plate and Brewster window. It is very difficult to adjust the focus exactly on the surface of the Al substrate immersed in liquid because of the refractive index of the medium the focal position extended towards the metal surface, which fabricate the nanoparticles at a poor rate. To get good rate of fabrication of nanoparticles the focus should be placed on the surface of the Al substrate. Not only the nanoparticles but the structure formation also depended on the position of the focus. The beam waist estimated at the focus was ~15 μm. Initially the level of liquid was ~2-3 mm above the Al sample. Al targets were placed normal to the laser beam on a motorized X-Y stage, which can be operated through the motion controller. Typical pulse energies used were ~250 μJ. The scanning speeds of the X-Y stages were 0.2 mm/sec and 0.4 mm/sec. Both the stages were controlled by Newport ESP 300 motion controller. The motorized stages (Newport) were moved in such a way to write periodic line pattern on the Al sample, at a separation of ~150 μm. Time of exposure was about 5 minutes and each scan resulted in 20 periodic lines. As a first step we performed the ablation in water, CCl_4 and $CHCl_3$ for a fixed polarization (S-polarization) in both fs and ps domain. Secondly, ablation was carried out in water for S, P and circular polarizations. Finally, ablation was performed in water only

for different levels of the water above the Al substrate. We compared the structure formed on the Al substrate below, near the ablation threshold and above the ablation threshold, for different water levels only in fs domain. The position of the focus was approximated to lie at the point where plasma was generated when it focused in air. Taking this as the confirmation we could manually change the position of the focus beyond the sample and exactly on the surface of the sample using a translational stage (along Z-direction) on which sample was fixed. We observed that the CCl_4, $CHCl_3$ and DCM solutions changed to gold-yellow color due to dispersion of ejected Al nanoparticles into the liquid[16] irrespective of the polarization. But water and Cyclohexane did not suffer any change in coloration in all of the three studies mentioned above, probably due to aggregation effects. Stratakis et al. reported[17] that the rate of NPs generation with 40 fs laser pulses at 800 nm is extremely low. This is mostly due to the fact that the peak power is so high that laser radiation is strongly absorbed by the liquid itself through non-linear processes. As a result, the fraction of laser energy that finally reaches the surface of the target is very small. The coloration of the NPs colloidal solution of Chloroform was thicker (dark yellow) than CCl_4 colloidal solution. The morphology of NPs was characterized by Transmission Electron Microscopy (TEM), FESEM (Ultra 55 from Carl ZEISS) analysis and the optical absorption spectra of the different colloidal solutions were recorded in the range of 200-600 nm with UV-Vis absorption spectrometer, Electron Diffraction Pattern and we observed that the coloration of the laser exposed portion on the metal changed to yellow color. FESEM images of the laser exposed portions in the Al substrate were showing different structure formations as previously reported mushroom structures by Stratakis et al.[16, 17].

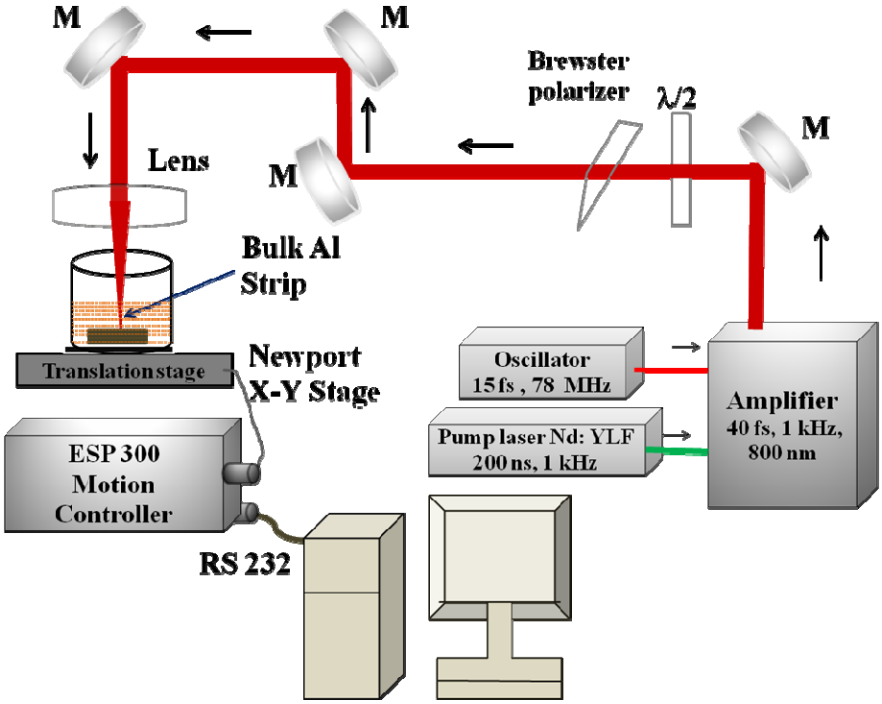

Figure 1 Experimental schematic of FLA schematic and similarly Picosecond.

RESULTS AND DISCUSSION

The colloidal solutions obtained by ablation of an Al target with two types of lasers (fs and ps) are different in appearance; the colloids produced with fs laser ablation look yellow in transmission, while those obtained with ps radiation look gray at higher fluence (~2-3 J/cm^2) and yellow at lower fluence (~1 J/cm^2). The coloration[18] of the colloidal solution is determined by the dielectric function of the liquid medium (along with dielectric function of the metal) in which ablation took place and laser parameters such as wavelength and pulse duration used. In both cases the solutions were slightly opalescent and their opalescence increased upon increasing the laser fluence. All the colloids prepared were stable against sedimentation for at least several months with no addition of any surface-active substances. This coloration could be assigned to structuring of Al surface and similar nanostructures were

previously reported in Ag and Au.[14, 19] Ablation of the same Al target in purified water, at fluencies of 2–3 J/cm^2, led to opalescent colorless solutions. This could be attributed to the chemical interaction of molten Al with water. The UV-Vis extinction spectra of the colloidal solution exhibited 300 nm peak for CCl_4 and at ~235 nm and ~270 nm peaks for $CHCl_3$ in fs domain.[20] In the ps domain [shown in figure 2(a)] the surface Plasmons exhibited peak at ~295 nm and peak at ~318 nm may be the bond dissociation peak for CCl_4. Figure 2(b) shows a ~320 nm single peak for $CHCl_3$.

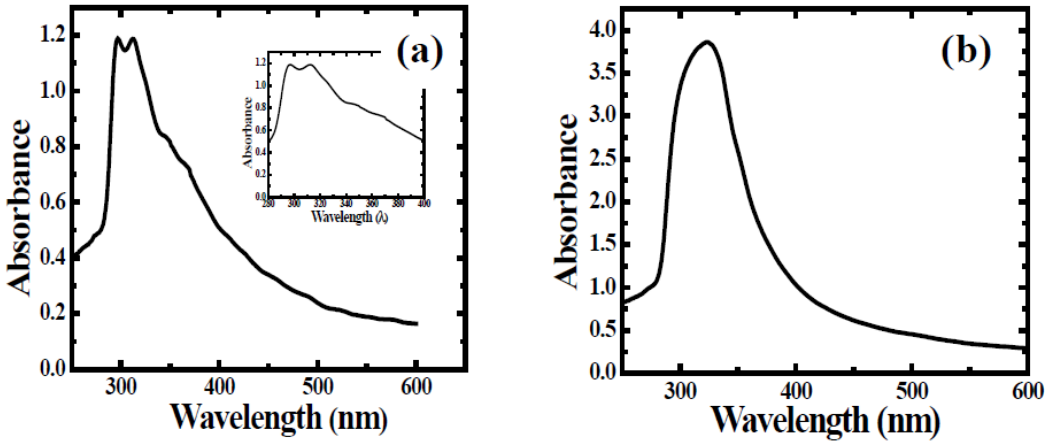

Figure 2 Absorption spectra of Al nanoparticles in (a) CCl_4 and (b) $CHCl_3$. Inset of (a) expanded view in the 280-400 nm range.

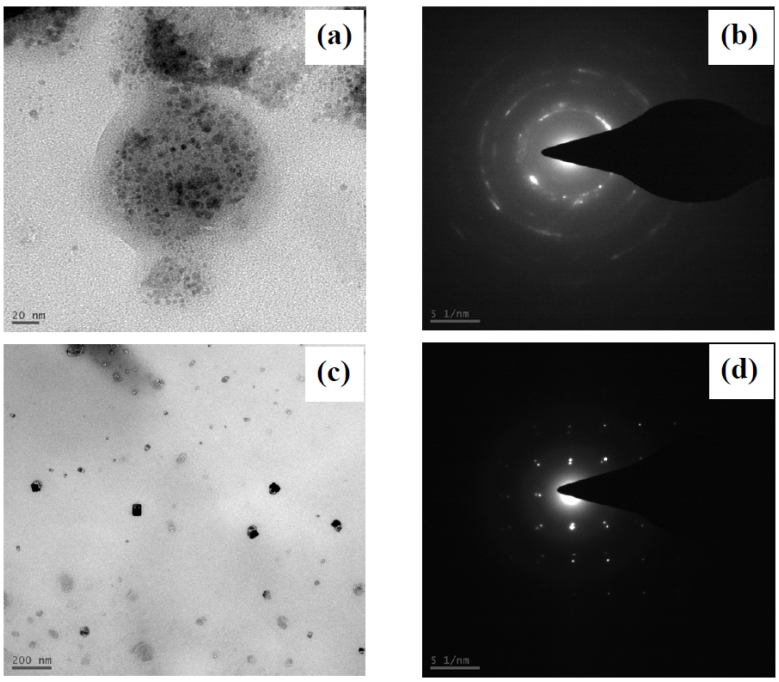

Figure 3 TEM view of nanoparticles generated via ablation of a bulk Al target in (a) CCl_4 & (c) $CHCl_3$ and Electron diffraction pattern of Al colloidal solution of (b) CCl_4 & (d) $CHCl_3$.

TEM image of the Al NPs produced by ps laser ablation is presented in figure 3(a) for the solvent CCl_4 and (c) for the solvent $CHCl_3$ indicating that a number of nanoparticles feature a tail. Figure 3(b) in CCl_4 and 3(d) in $CHCl_3$ represent the electron diffraction pattern and indicates they have mostly crystalline behavior. The NPs generated using ps laser pulses were more round in shape in CCl_4 and cubes in $CHCl_3$. The colloidal solution in this case

contained a significant amount of nanometer-sized debris[21] that envelope NPs. Such debris has low contrast upon imaging and is probably non-metallic.

The fs ablation was performed in water, CCl_4 and $CHCl_3$ for same input fluence (2-3 J/Cm^2) and for the same liquid level and polarization (S), well dispersed nanoparticles were observed in CCl_4 and $CHCl_3$ along with different grating formation on the substrates where as no nanoparticles was observed in water but structures on surface were observed. [20]

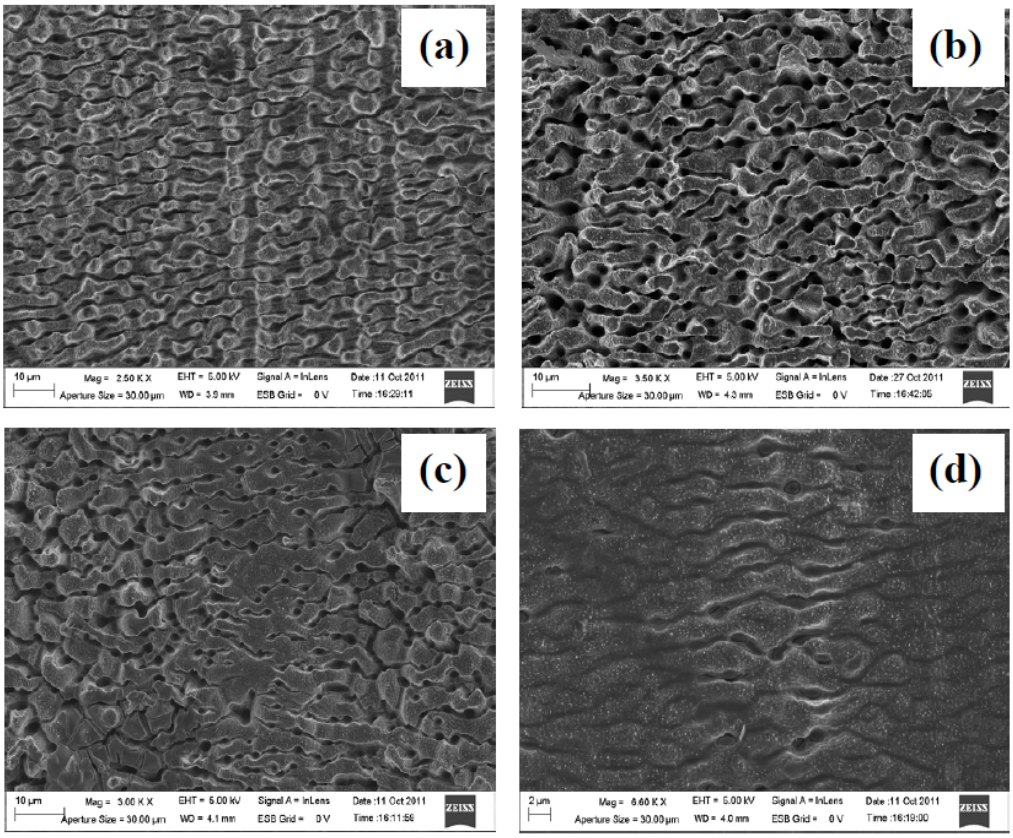

Figure 4 FE-SEM micrograph of micro structured surface prepared by ps laser ablation of Al into (a) water, (b) CCl_4, (c) $CHCl_3$ (at higher fluence) and (d) $CHCl_3$ (at lower fluence).

Microstructure or Coral structure[21] formation was observed when the fluence of the laser beam greater than the ablation threshold in figure 4 in water, CCl_4 and $CHCl_3$. When we place any liquid on the Al substrate, the refractive index of the liquid medium caused the focus to go beyond the sample. Even if the focus was beyond sample surface the fluence was greater than ablation threshold. For even higher fluences we observed a hole type micron structure [shown in figures 4 (a-c)] and for lower fluences (but still above the ablation threshold) periodic typed sub-micron (~0.6 μm) structures were observed and a typical structure is depicted in figure 4(d). Secondly, water level dependence of ablation above the Al substrate also demonstrated a different structure than mentioned above. We performed this in two ways (1) Ablation of Al for different levels of water by setting the fluence is below and near the ablation threshold. (2) Ablation for different levels of water by setting the fluence is above and more above the ablation threshold.

Particularly, in the first case we observed (nano-ripples) with a certain periodicity. FESEM images shown in figure 5 depicts the structures which were observed on the Al substrate immersed in water when the water level was 5 mm above the sample top surface implying that when the input fluence is decreased (but near to the ablation threshold)

nanostructures can be generated as shown in figure 5(a). When the level of water was 3 mm and 2 mm above the sample, the fluences increased above certain values and depending on material properties the ablated surface can organize in the form of nano-ripples. These are called laser-induced periodic surface structures (LIPSS)[22-26] with different periodicities ~330 nm and ~400 nm calculated using equation (1) and the structures are shown in figures 5(b) and 5(c), respectively. The interference of the incident electromagnetic wave with the surface electromagnetic wave (SEW) generated on the Al substrate could be the reason for these nanoripples. The closer view of these ripples demonstrated mushroom like nanostructures, tentatively assigned to Rayleigh-Taylor like instabilities which probably occurred between vapor of the liquid and the metal melt. Under the above mentioned instabilities redistribution of the melt might take place and hence mushroom like structures were observed[13].

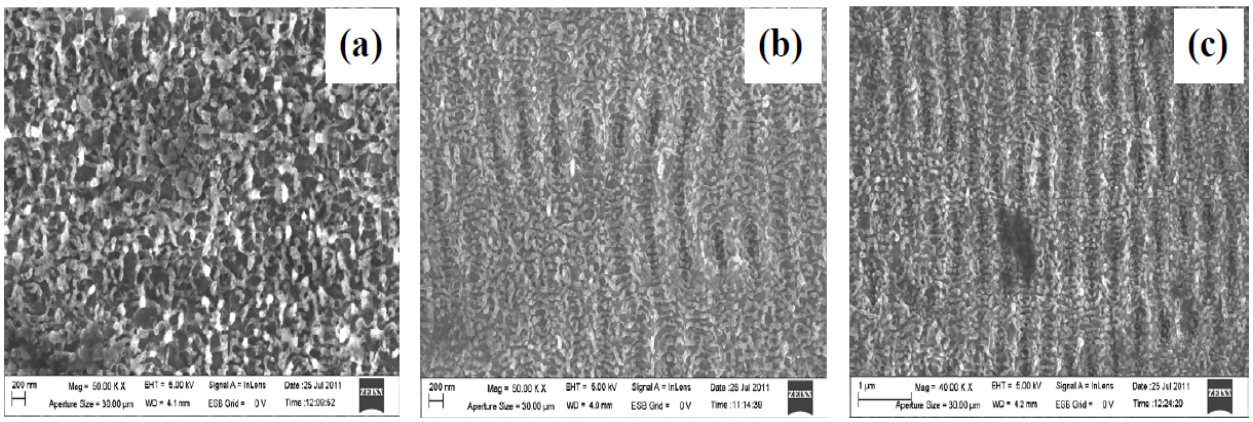

Figure 5 Different forms of self organized structures generated with fs laser pulse of Al in water (a) nanostructure (5 mm above), (b) 3 mm above and (c) LIPSS (Laser induced periodic surface structure) 2mm above.

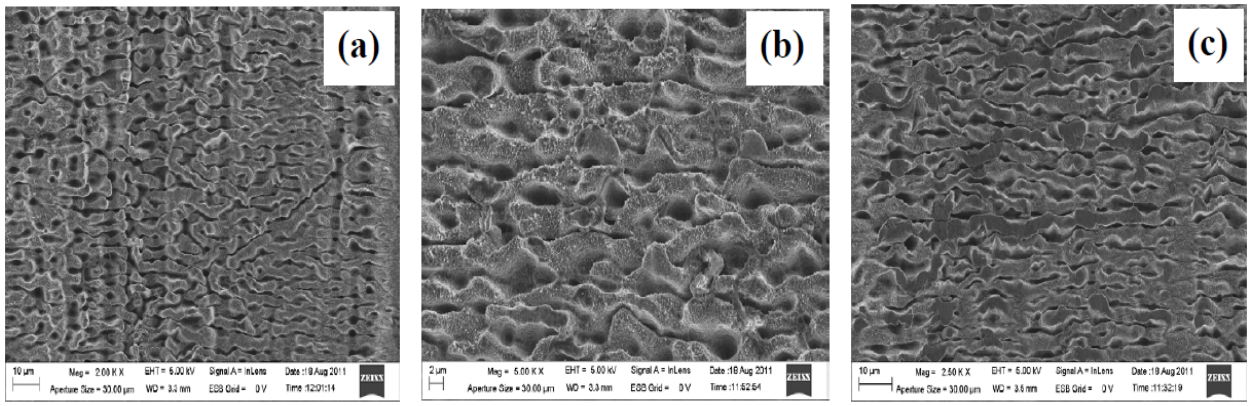

Figure 6 FE-SEM images of different forms of Microstructure (Coral Structure) (a) 5 mm above, (b) 3 mm above and (c) 2 mm above.

The periodicity (Λ) of nano-grating is given by the equation

$$\Lambda = \lambda / [(\lambda/\lambda_s) + \sin\theta_{in})] \quad (1)$$

Where λ is the incident laser wavelength, λ_s is the wavelength of surface electromagnetic wave, θ_{in} is the angle of incidence. When $\theta_{in} = 0$, periodicity will be equal to the wavelength of surface electromagnetic wave. ($\Lambda = \lambda_s$)

Micro-grating formed for different levels of liquid are shown in figure 6 with different liquid levels measured from the Al top surface. When number of pulses and fluence increased above the values where LIPSS appear, then the material surface started to self organize in micrometer range which is depicted in figure 6. Again the size and shape of these randomly assembled micro-size structures[27-30] can be controlled with input laser parameters. Beyond these structures, further increase of fluence and number of pulse led to the total evaporation of the material.

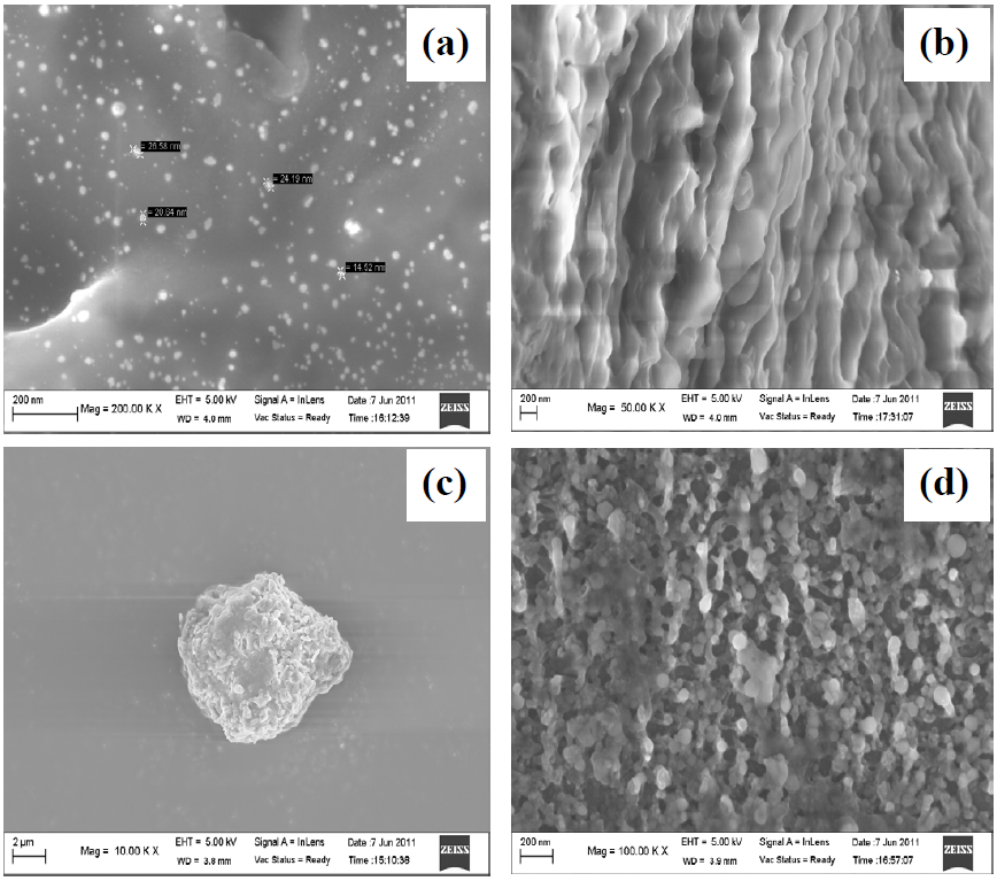

Figure 7 FESEM view of (a) nanoparticles in liquid and (b) periodic nanostructures on substrate was generated in DCM, and (c) clusters are formed (micron size) in liquid and (d) nanostructures on substrate in Cyclohexane.

In the fs domain, we observed the well dispersed Al nanoparticles in DCM and micron sized clusters in Cyclohexane colloidal solutions as shown in figures 7(a) and 7(c). In Cyclohexane nanoparticles aggregated to form clusters. Near the ablation thresholds nano-grating and nanostructures were observed on Al substrates in DCM and Cyclohexane as shown in figures 7(b) and 7(d), respectively. The main motivation behind the fabrication of the Al nano particles and nanostructures is to get the enhanced Raman signals from the trace molecules especially the explosive molecules[31] since the main source of SERS signal is either the colloidal solutions of the metallic nanoparticles or patterned surface of Nobel metals/coated metal surfaces with Nobel metals. Our future studies will focus on a systematic investigation of the structure period with laser energy, wavelength (400 nm ablation), etc.

CONCLUSIONS

In summary, ps and fs laser ablation of bulk Al sample in oxygen free liquid media like CCl_4 and $CHCl_3$ in an open air environment led to Al nanoparticle generation and structure formation. In fs domain, generation of both micro

and nano-structures depended on the ablation threshold. We could also generate nanoparticles of different sizes and size distribution in these solvents. Nonlinear optical properties of these nanoparticles are in progress. The nano-structures will be useful in enhancing the Raman signal (in Surface Enhanced Raman Scattering experiments) since these are involved with surface plasmons which are the collective vibrational modes of conduction electrons on the surface.

ACKNOWLEDGEMENTS

This work is supported by DRDO, India.

REFERENCES

[1] Chen, C. K., de Castro, A. R. B. and Shen, Y. R., "Surface Enhanced Second Harmonic Generation", Phys. Rev. Lett. **46**, 145 (1981)

[2] Wokaun, A., Bergman, J. G., Heritage, J. P., Glass, A. M., Liao, P. F. and Oslon D. H. "Surface Second Harmonic Generation from metal island films and micro lithographic structures" Phys. Rev. B **24**(2), 849-855 (1981).

[3] Garcia-Vidal, F. J., and Pendry, J. B., "Collective Theory for Surface Enhanced Raman Scattering" Phys. Rev. Lett. **77**, 1163 (1996).

[4] Cao, Y. W. C., Jin, R. C., and Mirkin, C. A., "Nanoparticles with Raman Spectroscopic finger prints for DNA and RNA detection", Science **297**, 1536 (2002).

[5] Fritzsche, W. and Taton ,T. A., "Metal nanoparticles as labels for heterogeneous, chip-based DNA detection" Nanotechnology **14**, R63-R73 (2003).

[6] Eliezer, S., Eliaz, N., Grossman, "E., Nanoparticles and nanotubes induced by femtosecond laser", Laser and particle beams 23, 15-19 (2005).

[7] Link, S., M.A. El- Syed, "optical properties and ultrafast dynamics of metallic nanocrystals", Annu. Rev. Phys. Chem. **54**, 331-366 (2003).

[8] Eliezer, S., Eliaz, N., Grossman, E., "Synthesis of nanoparticles with femtosecond laser pulses", Phys. Rev. B **69**, 144119-144125 (2004).

[9] Shafeev, G. A., Nova Science Publishers Inc, **1** (2008).

[10] Stratakis, E., Zorba, V., Barberoglou, M., Fotakis, C., and Shafeev, G.A., "Laser writing of nanostructures on bulk Al via its ablation in liquids", Nanotechnology **20**(10), 105303-105310 (2009).

[11] Radziemski, J. and Creamers, D.A., Laser Induced Plasma and Applications (Marcel Dekker, New York, 1989.

[12] Tilaki, R.M., Irajizad, A., Mahdavi, S.M., "Stability, size and optical properties of silver nanoparticles prepared by laser ablation in different carrier medium", Appl. Phys A, **84**, 215 (2006).

[13] Kazakevich, P.V., Simakin, A.V., Shafeev G.A., "formation of periodic structures upon laser ablation of metal targets in liquids" Quantum Electronics **35**, 831 (2005).

[14] Zavedeev, E.V., Petrovskaya, A.V., Simakin, A.V., Shafeev, G.A., "Formation of nanostructures upon laser ablation of silver in liquids", Quant. Electron. **36**, 978 (2006).

[15] Suna, J., Simon, S.L., "The melting behavior of aluminum nanoparticles", Thermochima Acta **463**, 32 (2007).

[16] Stratakis, E., Zorba V., Barberoglou, M., Fotakis, C., Shafeev, G.A., "Femtosecond laser writing of nanostructures on bulk Al via its ablation in air and liquids", Appl. Surf. Sci. **255**, 5346 (2009).

[17] Stratakis, E., Barberoglou, M., Fotakis, C., Viau, G., Garcia, C., and Shafeev, G A., "Generation of Al nanoparticles via ablation of bulk Al in liquids with short laser pulses" Opt. Exp., **17**(15), 12650-12659 (2009).

[18] Wagener, P., Stephan, B., Nico, B., "Fabrication of nanoparticles and nanomaterials using laser ablation in liquids" Photonic international, 20-23 (2011)

[19] Lau Truong, S., Levi, G., Bozon-Verduraz, F., Petrovskaya, A.V., Simakin, A.V., Shafeev, G.A.," Generation of Ag nanospikes via laser ablation in liquid environment and their activity in SERS of organic molecules" Appl. Phys. A, **89**, 373 (2007).

[20] Gopala Krishna, P., Hamad, S., Sreedhar, S., Tewari, S. P., Venugopal Rao, S., "Fabrication and characterization of aluminum nanostructures and nanoparticles obtained using femtosecond ablation technique", submitted to Chem. Phy. Lett., 2011.
[21] Kaakkunen, J., "Fabrication of functional surfaces using ultrashort laser pulse ablation" Dissertations in Forestry and Natural Sciences No **45**.
[22] Reif, J., Varlamona, O., and Costache, F., "Femtosecond laser induced nanostructure formation: self-organization control parameters," Applied Physics A: Materials Science & Processing **92**, 1019–1024 (2008).
[23] Costache, F., Kouteva-Arguirova, S., and Reif, J., "Sub-damage threshold femtosecond laser ablation from crystalline Si: surface nanostructures and phase transformation," Applied Physics A: Materials Science & Processing **79**, 1429–1432 (2004).
[24] Tsukamoto, M., Asuka, K., Nakano, H., Hashida, M., Katto, M., Abe, N., and Fujita, M., "Periodic microstructures produced by femtosecond laser irradiation on titanium plate," Vacuum **80**, 1346–1350 (2006).
[25] Wu, Q., Ma, Y., Fang, R., Liao, Y., Yu, Q., Chen, X., and Wang, K., "Femtosecond laser-induced periodic surface structure on diamond film," Appl. Phys. Lett. **82**, 1703–1705 (2003).
[26] Vorobyev, A. Y., Makin V. S, and Guo, C., "Periodic ordering of random surface nanostructures induced by femtosecond laser pulses on metals," Journal of Applied Physics **101**, 034903 (2007).
[27] Semaltianos, N. G., Perrie, W., P. French, Sharp, M., Dearden, G., and Watkins, K. G., "Femtosecond laser surface texturing of a nickel-based superalloy," Applied Surface Science, **255**, 2796– 2802 (2008).
[28] Ji-Ming, L. and Jian-Ting, X., "The evolution of a microstructure on Si by a femtosecond laser," Interaction of laser radiation with matter" **18**, 1539–1543 (2008).
[29] Kaakkunen, J.J.J., Paivasaari, K., Silvennoinen, M., Kuittinen, M., and Jaaskelainen,T. J, "Fabrication of the functional microstructures using focused femtosecond pulses," in Proceedings of LAMP2009 - the 5th International Congress on Laser Advanced Materials Processing (2009).
[30] Silvennoinen, M., Kaakkunen, J.J.J., Paivasaari, K., Vahimaa, P., and Jaaskelainen, T. J, "Controlling the Hydrophobic Properties of Material Surface Using Femtosecond Ablation," Journal of Laser Micro/Nanoengineering **5**, 97–98 (2010).
[31] Schmidit, M. S., Kostesha, N., Bosco, F., Olsen, J. K., Johnsen, C., Nielsen, K. A., "Xsens: using nanotechnology to combine detection methods for high sensitivity handheld explosive detectors", Proc. SPIE **7664**, 76641H1-6 (2009).